Brucella pituitosa strain BU72, a new hydrocarbonoclastic bacterium through exopolysaccharide-based surfactants production

Mouna MAHJOUBI
Univ. Manouba, ISBST, BVBGR-LR11ES31, Biotechpole Sidi Thabet

Hanene CHERIF
Univ. Manouba, ISBST, BVBGR-LR11ES31, Biotechpole Sidi Thabet

Habibu ALIYU
Karlsruhe Institute of Technology

Habib CHOUCHANE
Univ. Manouba, ISBST, BVBGR-LR11ES31, Biotechpole Sidi Thabet

Simone CAPPELLO
Istituto per l'Ambiente Marino Costiero (IAMC)-CNR of Messina. Sp. San Raineri

Mohamed NAIFER
Univ. Manouba, ISBST, BVBGR-LR11ES31, Biotechpole Sidi Thabet

Francesca MAPELLI
DeFENS- University of Milan

Yasmine SOUISSI
German University of Technology

Sara BORIN
DeFENS- University of Milan

Don A. COWAN
University of Pretoria

Ameur CHERIF
ameur.cherif@uma.tn

Univ. Manouba, ISBST, BVBGR-LR11ES31, Biotechpole Sidi Thabet

Research Article

Additional Declarations: No competing interests reported.

Abstract

Hydrocarbons and heavy metals pollution is considered among the most prevalent and serious problems in environment due to their toxicity and persistence. Bioremediation, using microorganisms, is considered as one of the most effective ways to reduce this type of pollution. In the present study, we unveil the bioremediation potential of *Brucella pituitosa* strain BU72. Besides its ability to grow on multiple hydrocarbons as sole carbon source and highly tolerant to several heavy metals, BU72 was able to produce different exopolysaccharide-based surfactants (EBS) when grown with glucose or with crude oil as sole carbon source. These EBS demonstrated particular and specific functional groups as determined by Fourier transform infrared (FTIR) spectral analysis that showed a strong absorption peak at 3250 cm^{-1} generated by -OH group for both EBS. The major differences in the FTIR spectra, of EBS produced are the increase of functional groups and the protein content. To better understand the EBS production coupled to the degradation of hydrocarbons and heavy metal resistance, the genome of strain BU72 was sequenced. Annotation of the genome revealed the presence of multiple genes putatively involved in EBS production pathways coupled with resistance to heavy metals genes such as arsenic tolerance and cobalt-zinc-cadmium resistance were identified. The genome sequence analysis showed the potential of BU72 to synthesize secondary metabolites and confirmed the presence of genes involved in plant-growth promoting. Here we provide a physiological and metabolic characterization associated with genomic analyses of BU72 considered as a promising candidate for application in the bioremediation.

Introduction

The widespread industrialization including petroleum industries emit various toxic heavy metals that are considered as environmental pollutants due to their toxicity, persistence and bioaccumulative nature. Petroleum pollution is a serious environmental problem due to their toxicity, carcinogenicity and mutagenic properties of petroleum components (Mahjoubi et al. 2013; Logeshwaran et al. 2018; Mahjoubi et al. 2018). Polycyclic aromatic (PAHs) constitutes one of the main components of crude oil and have been identified as hazardous compounds due to their recalcitrant, bioaccumulative and semi-volatile organic properties (Kappell et al. 2014; Alegbeleye et al. 2017). Several reports have demonstrated the certain human pathologies can be related to hydrocarbons and heavy metals exposure, including encephalopathy, arrhythmia and dermatitis (Sany et al. 2014; Tormoehlen et al. 2014). Moreover, the non-biodegradability of heavy metals promotes their prolonged presence in the environment (Gupta and Diwan 2017). Therefore, an efficient solution for the treatment of toxic compound such as heavy metals and hydrocarbons in the marine environment has become an urgent need. Bioremediation is considered as an alternative and effective technology for the treatment of oil-contaminated environments, especially marine habitats (Kimes et al.; 2014; Santisi et al. 2015). Effective bioremediation is dependent on the catabolic activities of microorganisms. Numerous microorganisms across all three domains have been reported in the bioremediation of contaminated environment, although the majority of such studies have focused on bacteria such as *Alcanivorax, Oleiphilus, Oleispira, Thalassolituus, Cycloclasticus* and *Ochrobactrum.* This latter was able to degrade a high number of pollutants including organophosphorus pesticides, phenol compounds, and petroleum (Head et al. 2006; Kimes et al. 2014; Talwar et al. 2014; Jamal and Pugazhendi 2018; Ortega-Gonzalez et al. 2018).

Several microorganisms produce various substances that enhance the bioremediation processes such as biosurfactant, bioemulsifiers, enzymes and exopolysaccharides (Ibrahim et al. 2020).

In addition, exopolysaccharide (EPS) possess several potential uses such as in nutrition, pharmaceutical, and chemical industries (Yaşar Yildiz et al. 2019) and are considered as efficient substances produced by oil-degrading bacteria to emulsify petroleum hydrocarbons (Ramasamy et al. 2014). EPS can increase solubilization of hydrocarbons and enhance degradation (Ramasamy et al. 2014). Also, EPS ensure bacterial survival under pollution condition including resistance to toxic agents, like heavy metals (Ibrahim et al. 2020). Several microorganisms, fungi, algae, or bacteria can remove toxic heavy metals through their EPS molecules produced (Mohite et al 2017). Therefore, the use of the microbial EPS is an effective biotechnological approach for heavy metal bioremediation.

In the last decade, several EPS producing microorganisms have been reported such as *Paenibacillus elgii, Serratia ficaria, Klebsiella mobilis, Kocuria rosea, Brevibacillus thermoruber* and *Ochrobactrum anthropic* (Ramasamy et al. 2014; Castellane et al. 2017; Chouchane et al. 2018; Ziervogel et al. 2019). Recent studies revealed that EPS-producing bacteria can utilize hydrocarbons as the sole carbon and energy source such as *Rhodococcus* that can utilize efficiently n-hexadecane and degrade linear and branched alkanes via biosurfactant or bioflocculant production. Members of the genus *Ochrobactrum* are well known for their abilities to degrade hydrocarbon (Chai et al. 2015; Chudasama and Thaker 2017). *Ochrobactrum*, an obligatory aerobic heterotrophic gram-negative member of the class Alpha-proteobacteria, has been isolated from diverse habitats (Huber et al. 2010; Yang et al. 2013; Chai et al. 2015). Recently, a study proved the ability of *Ochrobactrum pseudintermedium* to produce a surfactant EPS that was successfully used in bioremediation of waste lubricating and crude oil and in the biosorption of heavy metals (Sengupta et al. 2020). Similarly, Ramasamy et al., 2014 showed that *Ochrobactrum anthropic* is able to produce EPS that enhanced the degradation of hydrocarbons.

On the other hand, recently, the classification of Alphaproteobacteria was performed based on genomic analysis and that include *Ochrobactrum* in *Brucella* genus (Hördt et al. 2020). The genus *Brucella* encompasses 21 validly published species, which are available at https://lpsn.dsmz.de/genus/ochrobactrum. At today (August 2023), the NCBI database indicated the presence of 59 assembled *Brucella* genomes (https://www.ncbi.nlm.nih.gov/assembly). The search for new producing biosurfactants and EPS microorganisms is important to lead an effective bioremediation treatment. Very little is known about the bioremediation potential and the genome analysis of *Ochrobactrum* strains (Yang et al. 2013; Chudasama and Thaker 2017; Zarinviarsagh et al. 2017), therefore, this study aims to characterize *Brucella* (synonym *Ochrobactrum*) BU72 strain isolated from a chronically hydrocarbon-polluted sediment from Tunisia with a focus on its production of EPS, resistance to heavy metals, degradation of hydrocarbon and genome sequencing. By examining these features, the study will facilitate the comprehensive understanding of the *Brucella* strain capabilities and potential applications in bioremediation.

Material and Methods

Bacterial strain isolation, cultural and morphological characteristics

Brucella strain BU72 used in this study was isolated from a chronically hydrocarbon-polluted sediment from the Bizerte coast of northern Tunisia. The strain was isolated on mineral medium BHMS supplemented with 1% crude oil as the sole carbon source (Mahjoubi et al. 2013).

Growth of BU72 strain at different pH values (5–11) and salinity values (0, 5, 10, 15, 25, 30% w/v NaCl) was performed on TSA medium.

The ability of BU72 to utilize various hydrocarbons (phenanthrene, pristane, carbazole, pyrene, naphtalene, octadecane, fluoranthene, dibenzothiophene, dibenzofuran, squalene and anthracene) as a sole carbon and energy source was tested. BU72 was inoculated on mineral agar media ONR7a contained (per liter of distilled or deionized water) 22.79 g of NaCl, 11.18 g of $MgCl_2*6H_2O$, 3.98 g of Na_2SO_4, 1.46 g of $CaCl_2$, 2 H_2O, 1.3 g of TAPSO, 0.72 g of KCl, 0.27 g of NH_4Cl, 89 mg of $Na_2HPO_4 * 7 H_2O$, 83 mg of NaBr, 31 mg of NaHCO3, 27 mg of H_3BO_3, 24 mg of $SrCl*6H_2O$, 2.6 mg of NaF, and 2.0 mg of $FeCl_2*4H2O$, supplemented with specified amounts of previous hydrocarbons and incubated for 10 days at 28 ± 1˚C. Growth of the bacterial colonies was considered as positive result of degradation (Mahjoubi et al. 2021).

Production and characterization of EPS

Two media were used to study the production of EPS by BU72: 1) TSB supplemented with 10 g/l glucose, and 2) ONR7a supplemented with 1% crude oil. BU72 was grown on these two media at 28°C for 24 h. BU72 strain was cultivated in 250 mL flasks containing 100 mL of culture medium and incubated at 28°C with shaking for 4 days (TSB) and 15 days (ONR7a). To obtain the purified EPS, cultures were centrifuged to remove the cells by centrifugal separation (12,000 rpm/min, 20 min). Then, two volumes of cold ethanol were added to the supernatant and left overnight at 4°C. The precipitate was lyophilized to obtain the EPS fraction. Fourier transform infrared (FTIR) spectroscopy was used to determine the functional groups of the EPS as described before (Chouchane et al. 2018).

The phenotypic characterization of Exopolysaccharide Production was evaluated by cultivating the strains on Congo Red Agar (CRA) that allows the detection of exopolysaccharide production by variation in the color of colonies in the medium. The medium was prepared by adding 0.8 g of the Congo red dye in 1L of the tested media (ONR7a with crude oil and TSA with glucose). The bacterial isolates were streaked onto Congo Red Agar plates and incubated at 30°C for 48 hours.

Hydrocarbons utilization and crude oil degradation potential of BU72

To assess the capacity to utilize hydrocarbons, BU72 was cultured by inoculating 100 µl of microbial cells (~ 10^6 cells ml^{-1} measured by the DAPI count method) into 50 mL of ONR7a liquid mineral medium (Santisi et al. 2015) supplemented with crude oil (1%, v/v) as the sole carbon and energy sources. Incubation was performed at 28°C for 7 days. Culture growth was measured my monitoring turbidity), compared to non-inoculated controls. The composition of Total Extracted and Resolved Hydrocarbons (TERHCs) were analyzed chromatograph (Master GC, DANI Instruments, Milan, Italy), equipped with Split Splitless injector and flame-ionization detector (GC-FID) (DANI Master GC Fast Gas Chromatograph System, DANI Instruments S.p.A., Milan). The indices used to evaluate the relative biodegradation of *n*-alkanes are *n*-C17/Pristane (*n*C17/Pr), *n*-

C18/Phytane (*n*C18/Ph). The degradation of TERCHs was expressed as the percentage of TERCHs degraded compared to non-inoculated controls (Crisafi et al. 2016).

Bacterial resistance to heavy metals

The bacterial resistance to heavy metals was carried out on TSA medium supplemented with increasing concentrations of heavy metals (50–1,500 mg/L). The tested heavy metals were mercury chloride ($HgCl_2$), iron sulfate ($FeSO_4$), potassium dichromate ($K_2Cr_2O_7$), copper sulfate ($CuSO_4$), disodium arsenate (Na_2HAsO4) and cobalt chloride ($CoCl_2$). The positive control was used by inoculating bacterial suspension on agar plates without metal. The spot inoculation method with 10 μl of bacterial culture suspension (OD_{600} = 0.6) was used in triplicate. Bacterial cultures were incubated for 48 h at 32 ∘C (Ouertani et al. 2020).

Characterization of BU72 by scanning electron microscopy and GFP Transformation

For scanning electron microscopy, BU72 cultures were grown in Tryptic Soy Broth (TSB) for 48 at 28°C until exponential growth phase (OD600 around 0.5). Preparations for scanning electron microscope were performed according to Stanton et al. (2013). Cultures was were/was centrifuged and bacterial biomass was fixed in 2.5% glutaraldehyde in K-phosphate buffer (0.075 M, pH 7.4) for 2 h at room temperature. Samples were rinsed three times and fixed in 0.5% aqueous osmium tetroxide for 2h at room temperature. The dehydration of samples was performed in ethanol at concentrations of 30%, 50%, 70%, 90% and 3 × 100% for 10 min each. The Scanning Electron Microscope (SEM) used was a JCM-5700SEM, resolution 0.6 nm, specimen size 5 mm dia x 0.6 mm high, heating (1200°C) and cooling (N2(l)) stages, Gatan Digital Micrograph imaging system, SE & BS detectors (Stanton et al. 2013).

For the adheration to crude oil, the strain was preliminary tested for antibiotic resistance and the ability to growth on selective media. Strain BU72 could be suitable for the genetic transformation using broad host range plasmids. BU72 was transformed by electroporation. Competent cells of the bacterium were prepared as described by Mostafa et al. (2002). For the electroporation procedure, a mix of competent cells with pHM2-GFP plasmid (0.2-1 μg) was prepared, transferred into a cold 0.1-cm-diameter cuvette and pulsed at 1,700-2,000 V in the Electroporator apparatus. Transformants was checked and verified by PCR. After the transformation experiment BU72-GFP tagged strain was obtained, grown on diesel as unique carbon source and observed under fluorescence microscopy.

Genome sequencing and phylogenetic affiliation of BU72

DNA isolation was carried out on mid-log phase cells using sodium dodecyl sulfate (SDS)-proteinase K treatment with an additional equal volume of chloroform/isoamyl alcohol (24:1 v/v) (Mahjoubi et al. 2013). The concentration, purity (A260/A280 ratio), and absorbance ratio at 260–280 nm (A260/A230 ratio) were measured with a NanoDrop Spectrophotometer (NanoDrop™ 1000 Thermo Scientific). Genomic DNA was sequenced on an IlluminaMiSeq platform (MRDNA, Clearwater, Tx, USA). Read quality was accessed using PRINSEQ and reads were assembled using Spade 3.5 (Bankevich et al. 2012). The genome was annotated using the RAST pipeline (Aziz et al. 2008) and Integrated Microbial Genomes and Microbiomes (IMG/M) (Chen et al. 2023). The predicted protein sequences were functionally annotated using Clusters of Orthologous

Genes (COG) computed using the eggNOG-mapper (Huerta-Cepas et al. 2017). Analysis of the biosynthetic gene clusters was performed using AntiSMASH 7.0.0 tools (Blin et al. 2023).

The 16S rRNA gene sequence was predicted from the assembled genome using RNAmmer and phylogenetic trees were constructed using 16S rRNA gene sequences of the 21 sequenced *Brucella* strains obtained from the Ezbiocloud database (Yoon et al. 2017). The alignment was carried out using Mafft and gaps were removed using the default setting in Gblocks v.0.91b (Castresana, 2000). A phylogenetic dendrogram was constructed by the neighbor joining method and the tree topology was evaluated by performing bootstrap analysis of 1000 data sets using MEGA6.0 (Tamura et al. 2013). Species level taxonomic delineation was conducted by calculating average nucleotide identity (ANI) using OAT (version 0.93.1) (Lee et al. 2016) This analysis was carried out to compare the strain BU72 with its closest relatives, the *Brucella* strains, as well as to compare BU72 with the available *Brucella pituitosa* genomes. A heatmap was visualized using OAT (Lee et al. 2016) .

Proksee server was used for circular representation of multiple genomes (Grant et al. 2023). The draft genome of strain BU72 was used as the reference genome and was compared with genomes of *Brucella pituitosa* CCUG_50899, *Brucella rhizosphaerae* PR17, *Ochrobactrum quorumnocens* A44.

Results and Discussion

Morphological and phenotypic characterization of BU72

The hydrocarbonoclastic bacterium BU72 (GenBank accession number of 16S rRNA Sequence: KC153015) was isolated from hydrocarbon contaminated sediments from a refinery harbor of the Bizerte coast in Northern Tunisia and affiliated to *Ochrobactrum grignonense* (Mahjoubi et al. 2013). Isolation was performed on mineral medium supplemented with 1% crude oil as the sole carbon source. Stain BU72 showed the ability to produce biosurfactant and emulsification activity (Mahjoubi et al. 2013). BU72 was able to use various hydrocarbons as a sole carbon source including crude oil, phenanthrene, pyrene, naphthalene, octadecane, fluoranthene and anthracene. Whereas it was not classified as an obligate hydrocarbonoclastic bacterium, BU72 strain is considered as an heterotrophic bacterium with a capacity of using a wide range of hydrocarbons. Microscopic observation of the BU72- GFP visualizes the physical interaction of the bacterium with the diesel droplet (Fig. 1). The cells are adhering to the oil drop surface forming a patchwork of fluorescent microcolonies on the oil drop surface. Under Scanning electron microscopy, the bacteria are rod shaped and revealed a typical morphology of *Ochrobactrum* (Figure. 1) (Yu et al. 2019). Several reports demonstrated the biodegradation ability for the genus *Ochrobactrum* such as the degradation of phthalates, polyaromatic hydrocarbons, heavy metals and different classes of pesticides (Yirui et al. 2009; Pandey et al. 2013; Ghosal et al. 2016; Nayak et al. 2019; Onder Erguven and Demirci 2020).

The strain grew at pH range from 5 to 11 and tolerated salinity from 0–10%. In vitro experiments showed that BU72 strain produce exopolysaccharides and biosurfactant.

Heavy metal resistance experiments indicated that BU72 strain has the capacity to grow under high concentrations of arsenic (up to 2,500 mg/L), copper, chrome, cadmium and nickel (up to 1,000 mg/L), and Cobalt (up to 500 mg/L). Several studies have proven the resistance of *Ochrobactrum* to various heavy

metals. *Ochrobactrum anthropi* was reported in the adsorption of chromium(16 mg/ L), cadmium (30 mg/L) and copper ions (125 mg/ L) (Ozdemir et al. 2003). The inoculation of the iron-oxidizing strain *Ochrobactrum sp.* EEELCW01 into Arsenic polluted paddy soil, as a microbial agent, could effectively reduce As bioavailability (Qian et al. 2022) The minimum inhibition concentration of copper-resistant bacterium *Ochrobactrum* MT180101 was between 100 mg/L and 150 mg/L (Peng et al. 2019). Thus, *Ochrobactrum* exhibits a diverse range of metabolic capabilities which make these bacteria potential candidates for bioremediation strategies. The inoculation of hyper accumulator strain *Ochrobactrum tritici* As5 reduced the uptake of arsenic by the rice plants and alleviaties some of the toxic effects of arsenic on shoot length (Moens et al. 2020).

Exopolysaccharide-based surfactants (EBS) Synthesis

Structural analysis of both exopolysaccharide-based surfactants (EBS) was comparatively evaluated by Fourier Transform InfraRed (FT-IR) spectrometer (Fig. 2. a, b).

The results showed strong absorption peaks at 3250 cm^{-1} generated by -OH group (free hydroxyl group typical for carbohydrates) for both EBS. The absorbance peaks in the region 2900−2700 cm^{-1} (Fig. 2. b) and at 2800 cm^{-1} (Fig. 2. a) showed the presence of terminal methyl group of aliphatic stretching bands (CH, CH2, CH3) which are more abundant in EBS produced when BU72 was grown with crude oil as sole carbon source (figure. b). The presence of these groups is confirmed by bands observed around 1300−1400 cm^{-1}. The weak peak around 2200−2250 cm^{-1} indicates that both EBS contained $-C \equiv C-$ groups but more relevant in EBS produced in crude oil medium. The weak absorption located at 1800 cm^{-1} indicates that both EBS contained a low amount of acetyl group. The large peak at 1600 cm^{-1} indicates the presence of carbonyl $-C = O$ in the two EBS. Peaks at 1500 (Fig. 2. a) and 1550 cm^{-1} (Fig. 2. b) were attributed to -NH bending of amide groups and proteins more relevant in EBS produced in crude oil medium. The bands at 1250 and 1180 cm − 1 argued the availability of sulphated groups such as C = S. The peaks around 1050−900 cm^{-1} were reported as the characteristic peaks of sugar derivatives and uronic acid. The major differences in the FTIR spectra, of EBS produced in crude oil medium and EBS produced when glucose was used as carbon source, are the increase of functional groups and the protein content. These properties give the EBS a particular effectiveness to well bind hydrocarbon molecules and play critical role in the emulsification and dispersion of oil droplets.

It was reported that some surface-active compounds such as EPS, bioemulsifiers and biosurfactants are related with degradation of hydrocarbons (Castellane et al. 2017).

Ochrobactrum pseudintermedium was able to produce two types of EPS by utilizing different hydrocarbon substrates: a surfactant EPS (SEPS) and an emulsifier EPS (EEPS) (Sengupta et al. 2019). The carbon source was considered as a very significant factor influencing the nature and the physicochemical properties of bacterial EPS produced (Ibrahim et al. 2020).

*Halobacillus s*train EG1HP4QL was able to produce an extracellular polysaccharide that had significant emulsifying activity against kerosene (65.7 ± 0.8%), *o*-xylene (64.0 ± 1%), and sunflower oil (44.7 ± 0.5%). This strain was resistant to elevated concentrations of some heavy metals such as Cu, Pb, and Ni (Ibrahim et al. 2020). EPS producer may represent an excellent ecological alternative in numerous industrial fields and in bioremediation treatment.

Insights into the genome of BU72

The BU72 genome comprises 4,885,407 base pairs (bp) with a G + C content of 53.4%, assembled into nine scaffolds (Table 1). The circular map representing the *Brucella* BU72 genome is represented in Fig. 3. RAST annotation revealed that the genome contained a total of 4,765 genes, including 4,711 protein encoding sequences and 54 RNAs. Approximately, 74% of the predicted protein coding sequences (CDSs) (Table 2). Analysis of the complete 16S rRNA gene sequences revealed that *Ochrobactrum* BU72 showed highest sequence similarity (99.86%) with *Brucella pituitosa* strain CCUG 50899[T], Further, characterization of the genomic relatedness between BU72 and available genome of *Brucella pituitosa* (9 genomes) revealed that they share in silico OrthoANI similarities of > 98% suggesting that strain BU72 is classified as a strain of *Brucella pituitosa* (Fig. 4, Fig. 5).

Table 1
16S similarity of BU72 and closest type strains (EZBiocloud)

Hit taxon name	Hit strain name	Accession	Similarity
Brucella pituitosa	CCUG 50899(T)	AM490609	100.00
Brucella rhizosphaerae	PR17(T)	NNRK01000031	99.48
Ochrobactrum quorumnocens	A44(T)	MG835335	99.11
Brucella thiophenivorans	DSM 7216(T)	NNRJ01000011	99.03
Brucella grignonensis	OgA9a(T)	NNRL01000158	98.81
Brucella pseudogrignonensis	CCUG 30717(T)	NNRM01000012	98.74
Ochrobactrum teleogrylli	LCB8(T)	MK063698	98.22
Brucella cytisi	ESC1(T)	AY776289	98.22
Brucella anthropi	ATCC 49188(T)	CP000758	98.22
Brucella tritici	SCII24(T)	AJ242584	98.22
Brucella haematophila	CCUG 38531(T)	AM422370	98.14
Brucella pecoris	08RB2639(T)	FR668302	98.07

Table 2
Genome attributes of strain BU72

Attribute	value	% of total
Genome size (bp)	4885407	100
Scaffolds s	9	100
DNA G + C number of bases	2610347	53.43
Genes total number	4768	100
Protein coding genes	4661	97.76
RNA genes	59	1.24
Protein coding genes with function prediction	3862	81.
Protein coding genes without function prediction	799	16.76
Protein coding genes connected to KEGG pathways	3899	81.77
Protein coding genes with COGs	3163	2635
Protein coding genes with with Pfam	3945	82.74
NCBI Assembly Accession	SAMN08100214	
NCBI Bioproject Accession	PRJNA419894	

B. pituitosa genome BU72 showed the presence of genes encoding enzymes which are involved in the synthesis of glycolipid biosurfactant such as phosphomannomutase, glycosyl-transferase, dTDP-4-dehydrorhamnose reductase, dTDP-4-dehydrorhamnose 3,5-epimerase, Glucose-1-phosphate thymidylyltransferase and dTDP-glucose 4,6-dehydratase (Table 3).

Table 3
Enzymes involved in Heavy metals resistance, EPS and Biosurfactant production

Contig_id	feature_id	start	Stop	function
Arsenic resistance				
NZ_PHRE01000001.1	Figure 571256.30.peg.978	1010163	1010540	Arsenical resistance operon repressor
NZ_PHRE01000001.1	Figure 571256.30.peg.979	1010554	1011081	Arsenate reductase (EC 1.20.4.4) thioredoxin-coupled, LMWP family
NZ_PHRE01000001.1	Figure 571256.30.peg.980	1011081	1012139	Arsenical-resistance protein ACR3
NZ_PHRE01000001.1	Figure 571256.30.peg.981	1012139	1012552	Arsenate reductase (EC 1.20.4.1) glutaredoxin-coupled, glutaredoxin-like family
NZ_PHRE01000001.1	Figure 571256.30.peg.982	1012533	1013303	Arsenic resistance protein ArsH
NZ_PHRE01000001.1	Figure 571256.30.peg.992	1021205	1020858	Transcriptional regulator, ArsR family
Copper resistance				
NZ_PHRE01000001.1	Figure 571256.30.peg.625	671126	670581	Copper resistance protein CopD / Cytochrome c family protein
NZ_PHRE01000001.1	Figure 571256.30.peg.626	672396	671191	Copper resistance protein CopD / Cytochrome c family protein
NZ_PHRE01000001.1	Figure 571256.30.peg.627	672770	672411	Copper resistance protein CopC
NZ_PHRE01000004.1	Figure 571256.30.peg.2339	63992	64996	Conserved membrane protein in copper uptake, YcnI / Copper metallochaperone PCu(A)C, inserts Cu(I) into cytochrome oxidase subunit II
NZ_PHRE01000001.1	Figure 571256.30.peg.1479	1527473	1526667	Cytoplasmic copper homeostasis protein CutC
NZ_PHRE01000004.1	Figure 571256.30.peg.2602	330808	333282	Lead, cadmium, zinc and mercury transporting ATPase (EC 3.6.3.3) (EC 3.6.3.5); Copper-translocating P-type ATPase (EC 3.6.3.4)
NZ_PHRE01000004.1	Figure 571256.30.peg.2427	160542	158947	Apolipoprotein N-acyltransferase / Copper

Contig_id	feature_id	start	Stop	function
Arsenic resistance				
				homeostasis protein CutE
NZ_PHRE01000004.1	Figure 571256.30.peg.2428	161654	160542	Magnesium and cobalt efflux protein CorC
Zinc resistance				
NZ_PHRE01000004.1	Figure 571256.30.peg.2476	206156	206905	Zinc metalloprotease
NZ_PHRE01000001.1	Figure 571256.30.peg.162	170067	170855	Zinc ABC transporter, ATP-binding protein ZnuC
NZ_PHRE01000001.1	Figure 571256.30.peg.163	170852	171730	Zinc ABC transporter, permease protein ZnuB
NZ_PHRE01000001.1	Figure 571256.30.peg.164	171751	172686	Zinc ABC transporter, substrate-binding protein ZnuA
NZ_PHRE01000001.1	Figure 571256.30.peg.1485	1533058	1532132	Cobalt-zinc-cadmium resistance protein
Cobalt resistance				
NZ_PHRE01000001.1	Figure 571256.30.peg.1688	1758188	1757427	Cobalt ABC transporter, ATP-binding protein CbtL
NZ_PHRE01000001.1	Figure 571256.30.peg.1689	1759240	1758185	Cobalt ABC transporter, permease protein CbtK
NZ_PHRE01000001.1	Figure 571256.30.peg.1690	1760262	1759237	Cobalt ABC transporter, substrate-binding protein CbtJ
NZ_PHRE01000001.1	Figure 571256.30.peg.1485	1533058	1532132	Cobalt-zinc-cadmium resistance protein
NZ_PHRE01000001.1	Figure 571256.30.peg.1481	1529664	1527826	Zinc carboxypeptidase A metalloprotease (M14):ATP/GTP-binding site motif A (P-loop):Sigma-54 factor interaction domain:ABC tr
Chromate				
NZ_PHRE01000004.1	Figure 571256.30.peg.3204	939081	940391	Chromate transport protein ChrA
NZ_PHRE01000004.1	Figure 571256.30.peg.2766	497894	498445	Chromate reductase (EC 1.6.5.2)
Various other genes involved in heavy metals resistance				
NZ_PHRE01000004.1	Figure 571256.30.peg.3170	902776	903684	Cobalt-zinc-cadmium resistance protein

Contig_id	feature_id	start	Stop	function
Arsenic resistance				
NZ_PHRE01000004.1	Figure 571256.30.peg.2601	330727	330302	Transcriptional regulator, MerR family
NZ_PHRE01000004.1	Figure 571256.30.peg.2602	330808	333282	Lead, cadmium, zinc and mercury transporting ATPase (EC 3.6.3.3) (EC 3.6.3.5); Copper-translocating P-type ATPase (EC 3.6.3.4)
NZ_PHRE01000004.1	Figure 571256.30.peg.3569	1294252	1294638	Transcriptional regulator, MerR family
NZ_PHRE01000004.1	Figure 571256.30.peg.4659	2370099	2370548	Transcriptional regulator, MerR family
NZ_PHRE01000001.1	Figure 571256.30.peg.1481	1529664	1527826	Zinc carboxypeptidase A metalloprotease (M14):ATP/GTP-binding site motif A (P-loop):Sigma-54 factor interaction domain:ABC tr
NZ_PHRE01000004.1	Figure 571256.30.peg.4661	2375727	2373244	Lead, cadmium, zinc and mercury transporting ATPase (EC 3.6.3.3) (EC 3.6.3.5); Copper-translocating P-type ATPase (EC 3.6.3.4)
NZ_PHRE01000003.1	Figure 571256.30.peg.2221	131721	131206	Chromate transport protein ChrA
NZ_PHRE01000003.1	Figure 571256.30.peg.2222	131910	131749	Chromate transport protein ChrA
NZ_PHRE01000008.1	Figure 571256.30.peg.4844	699	1112	Mercuric transport protein, MerT
NZ_PHRE01000008.1	Figure 571256.30.peg.4845	1129	1416	Periplasmic mercury(+ 2) binding protein, MerP
NZ_PHRE01000008.1	Figure 571256.30.peg.4847	1686	3128	Mercuric ion reductase (EC 1.16.1.1)
NZ_PHRE01000008.1	Figure 571256.30.peg.4843	600	160	Mercuric resistance operon regulatory protein MerR
NZ_PHRE01000001.1	Figure 571256.30.peg.995	1023526	1025370	Lead, cadmium, zinc and mercury transporting ATPase (EC 3.6.3.3) (EC 3.6.3.5); Copper-translocating P-type ATPase (EC 3.6.3.4)
NZ_PHRE01000001.1	Figure 571256.30.peg.1229	1260605	1260036	transcriptional activator of exopolysaccharide II

Contig_id	feature_id	start	Stop	function
Arsenic resistance				
				synthesis, MarR family protein
NZ_PHRE01000001.1	Figure 571256.30.peg.1231	1262577	1263992	STRUCTURAL ELEMENTS; Cell Exterior; surface polysaccharides/antigens
NZ_PHRE01000001.1	Figure 571256.30.peg.1725	1795455	1796702	Exopolysaccharide production protein ExoF precursor
NZ_PHRE01000001.1	Figure 571256.30.peg.1117	1133213	1131957	exopolysaccharide production protein, putative
EPS Nucleotide Sugars Biosynthesis				
NZ_PHRE01000004.1	Figure 571256.30.peg.3002	732968	731949	Glucokinase (EC 2.7.1.2)
NZ_PHRE01000004.1	Figure 571256.30.peg.2335	60023	61654	Phosphoglucomutase (EC 5.4.2.2)
NZ_PHRE01000001.1	Figure 571256.30.peg.1241	1276104	1275226	dTDP-4-dehydrorhamnose reductase (EC 1.1.1.133)
NZ_PHRE01000001.1	Figure 571256.30.peg.1242	1277177	1276101	dTDP-glucose 4,6-dehydratase (EC 4.2.1.46)
NZ_PHRE01000001.1	Figure 571256.30.peg.1243	1277738	1277187	dTDP-4-dehydrorhamnose 3,5-epimerase (EC 5.1.3.13)
NZ_PHRE01000001.1	Figure 571256.30.peg.1244	1278619	1277735	Glucose-1-phosphate thymidylyltransferase (EC 2.7.7.24)
NZ_PHRE01000001.1	Figure 571256.30.peg.242	255420	254797	Glucose-6-phosphate isomerase, archaeal (EC 5.3.1.9)
NZ_PHRE01000001.1	Figure 571256.30.peg.1670	1734226	1732799	Mannose-1-phosphate guanylyltransferase (EC 2.7.7.13) / Mannose-6-phosphate isomerase (EC 5.3.1.8)
NZ_PHRE01000001.1	Figure 571256.30.peg.1671	1735662	1734223	Phosphomannomutase (EC 5.4.2.8)
NZ_PHRE01000001.1	Figure 571256.30.peg.1164	1181600	1180902	UTP−glucose-1-phosphate uridylyltransferase (EC 2.7.7.9)
NZ_PHRE01000004.1	Figure 571256.30.peg.4761	2479417	2480343	Fructokinase (EC 2.7.1.4)

Contig_id	feature_id	start	Stop	function
Arsenic resistance				
NZ_PHRE01000001.1	Figure 571256.30.peg.1575	1629399	1628092	Xylose isomerase (EC 5.3.1.5)
NZ_PHRE01000001.1	Figure 571256.30.peg.1576	1630896	1629445	Xylulose kinase (EC 2.7.1.17)
Biosynthesis of N eps				
NZ_PHRE01000004.1	Figure 571256.30.peg.4730	2443816	2446611	[Protein-PII] uridylyltransferase (EC 2.7.7.59) / [Protein-PII]-UMP uridylyl-removing enzyme
NZ_PHRE01000004.1	Figure 571256.30.peg.3635	1356228	1357376	Nitrogen regulation protein NtrB (EC 2.7.13.3)
NZ_PHRE01000004.1	Figure 571256.30.peg.3636	1357373	1358845	Nitrogen regulation protein NR(I), GlnG (= NtrC)
NZ_PHRE01000004.1	Figure 571256.30.peg.3637	1359003	1361318	Nitrogen regulation protein NtrY (EC 2.7.3.-)
NZ_PHRE01000004.1	Figure 571256.30.peg.3638	1361320	1362681	Nitrogen regulation protein NtrX
EPS Exportation				
NZ_PHRE01000004.1	Figure 571256.30.peg.2962	694939	695154	Type 1 capsular polysaccharide biosynthesis protein J
NZ_PHRE01000004.1	Figure 571256.30.peg.4731	2446630	2448219	Peptidoglycan lipid II flippase MurJ
NZ_PHRE01000001.1	Figure 571256.30.peg.1119	1134376	1135563	Glycosyltransferase
NZ_PHRE01000001.1	Figure 571256.30.peg.1703	1769528	1770472	Outer membrane autotransporter barrel
NZ_PHRE01000001.1	Figure 571256.30.peg.882	903707	901920	Inner membrane protein, KefB/KefC family
NZ_PHRE01000004.1	Figure 571256.30.peg.3969	1707092	1707682	Polysaccharide export protein
NZ_PHRE01000001.1	Figure 571256.30.peg.897	921116	919488	D-ribulokinase (EC 2.7.1.47)

Several genes potentially associated with EPS production were identified in the genome of BU72. Usually, the mechanism of EPS synthesis comprises three steps: i) the synthesis of nucleoside diphosphate sugars (NDP sugars), ii) polymerization of the repeat monomers, and iii) the translocation and secretion. In the genome BU72, we identified the Glucokinase that ensure the phosphorylation of the glucose on the D-glucose 6P. This latter is transformed to D-glucose 1P through the phosphoglucomutase. The D-glucose 1P converted to dTDP

glucose via the glucose- 1-phosphate thymidylytransferase. Then, the dTDP glucose 4.6 dehydratase catalyzes the dehydration of the dTDP glucose to dehydrated dTDP-4dehydro6deoxyglucose. The 4 dehydrorhamnose 3,5 epimerase covert the dTDP-4dehydro6deoxyglucose to dTDP-4 keto rhamnose which transform to dTDP rhamnose via dTDP 4 dehydrorhamnose reductase. Then, the D-glucose 6P is transformed to fructose 6P through via a glucose 6P isomerase (Table 3).

The regulation of the various EPS biosynthesis pathways differs amongst the bacterial species (Schmid et al. 2015). Several reports showed that nitrogen which is an important component for bacterial growth and hydrocarbon degradation, play a key role in the production of metabolites including biosurfactants and EPS (Chouchane et al. 2021). Then, for the enzymatic regulation of the biosynthesis EPS, several genes were detected in BU72 and related to the nitrogen regulatory mechanism including Protein-PII uridylyltransferase, Nitrogen regulation protein NtrC, Nitrogen regulation protein NtrB (EC 2.7.13.3), Nitrogen regulation protein NtrY (EC 2.7.3.-), Nitrogen regulation protein NtrX, polysaccharide export protein nLipopolysaccharide biosynthesis protein WzxC, Inner membrane protein, tetratricopeptide tpr_2 repeat protein Outer membrane autotransporter barrel (Table 3) .

The genome of BU72 was investigated to identify genes putatively involved in the resistance to heavy metals. The genome annotation of BU72 highlighted the presence of numerous genes involved in resistance to arsenic, copper, and zinc.

Several genes involved in zinc resistance were found in the genome of BU72 such as Zinc uptake regulation protein (zurR), Zn uptake protein-encoding genes (znuA) and export protein-encoding genes (znuABC). For arsenic detoxification, the most described system is resistance module system (ARS), which is represented by the presence of arsRDABC components. Five genes involved in Arsenic resistance were predicted in strain BU72 including ArsR, and genes encoding an $As3+$ efux pump (arsB) and an $As5+$ reductase (arsC), arsenical resistance protein (arsH) (Table 3).

Furthermore, the work of Sengupta et al (2021), demonstrated the effectiveness of a surfactant exopolysaccharide (SEPS) produced by *Ochrobactrum pseudintermedium* in adsorbing and remediating toxic heavy metals such as cadmium, nickel, and lead dissolved in water.

The metabolism of benzoate is considered as an important key in the degradation of various aromatic compounds. A number of enzyme-coding genes for benzoate degradation were identified in BU72 genome, inclusing4-carboxymuconolactone decarboxylase [EC:4.1.1.44]; 3-hydroxybutyryl-CoAdehydrogenase [EC:1.1.1.157]; catechol 2,3-dioxygenase [EC:1.13.11.2]; acetyl-CoA C-acetyltransferase [EC:2.3.1.9] and glutaryl-CoA dehydrogenase [EC:1.3.8.6]. These enzymes are known to be involved in polyaromatic hydrocarbon degradation and are common in hydrocarbonoclastic bacteria (Palet al. 2017). Chudasama et al. (2017) reported that the genome of *Ochrobactrum anthropi* strain SUBG007 contains a large number of genes responsible for the degradation of xenobiotic compounds such as benzoate biphenyl, toluene and xylene, naphthalene and anthracene.

Several others genes which are involved in oil degradation were detected in the genome BU72 as those implicated in the metabolism of chloroalkane and chloroalkene via Alcohol dehydrogenase. This key enzyme

was also described in the genome of *Franconibacter pulveris* which is responsible for chloroalkane and chloroalkene degradation (Pal et al. 2017).

The annotation of BU72 genome showed multiple genes involved in stress- adaptation such as osmotic stress (32 genes), oxidative stress (48 genes) and to heat stress (16 genes) and cold stress (6 genes).

The genome BU72 has been well characterized and devoid of bacterial virulence gene such as virB operon. *Brucella* and *Ochrobactrum* have distinct pathogenic lifestyles, with *Ochrobactrum spp.* being generally considered to have low virulence (Hördt et al. 2020; Ryan and Pembroke 2020; Yagel et al. 2020). The study of Yagel et al. (2020) identified a limited number of virulence factors in the majority of *Ochrobactrum* genome (130 whole-genome sequences of *Ochrobactrum*).

Secondary metabolites prediction and plant-growth promoting trait genes

Based on antiSMASH analyses of BU72 genome, seven gene clusters related to the biosynthesis of secondary metabolites were predicted, including *N*-acetylglutaminylglutamine amide (NAGGN), Non-alpha poly-amino acids like e-Polylysin (NAPAA), siderophore, betalactone, acyl amino_acids, terpene, arylpolyene (Table 4, Supp Fig. 1).

Table 4
The prediction of Biosynthetic Gene Clusters from AntiSMASH

Region	Position		Cluster type	Type Most similar known cluster
	From	To		
Region 3.1	51,556	72,528	NAGGN	galactoglucan
Region 4.1	236,458	270,645	NAPAA	
Region 5.1	207,107	221,801	NI-siderophore	ochrobactin
Region 12.1	75,687	103,511	betalactone	corynecin III /corynecin I/corynecin II
Region 13.1	35,057	95,803	acyl amino_acids	•ambactin NRP
Region 13.2	862,784	883,617	terpene	
Region 13.3	889,117	930,298	arylpolyene	TVA-YJ-2/ RiPP

The siderophore identified in BU72 was ochrobactin, which may act as a biocontrol agent in plants by reducing the iron availability for phytopathogens (Lee et al. 2020). It has been identified in various bacterial species such as *Brucella anthropi* strain T16R-87. These siderophores play a crucial role in facilitating iron uptake in iron-limited environments which may contribute to the promotion of plant growth under environmental stresses. The genome of BU72 encode proteins involved in the production of an N-acetylglutaminylglutamine amide (NAGGN) which is a potent osmoprotectant conferring bacterial cells with resistance to osmotic stress (Kotecka et al. 2021). This compound was detected in osmotically stressed cultures of *Pseudomonas*

aeruginosa, and at higher NaCl concentrations, NAGGN became the dominant osmolyte in *Pseudomonas aeruginosa* (D'Souza-Ault et al. 1993; Aspedon et al. 2006).

Beta-lactones and terpene were also predicted in BU72 genome. These compounds exhibit anti-microbial effects and might be involved in defense mechanisms and it was detected in several bacterial species such as *Streptomyces, Myxobacteria, Pseudoruegeria* (Cho et al. 2020).

In addition, the annotation of the draft genome sequence confirmed the presence of genes involved in plant-growth promoting including in Phosphate metabolism, Ammonia assimilation, Auxin biosynthesis and proline Synthesis (Supp Table 1). The potentiel of *Ochrobactrum sp* CdSP9 for bioremediation by reducing the toxic effect of metal an inducing the germination and plant growth when applied to rice as host plant. The work of Pandey et al. (2013) indicated that *Ochrobactrum sp* CdSP9 constitute a promise candidate for bioremediation as well as for plant growth promotion by reducing the toxic effect of metal an inducing the germination and plant growth when applied to rice as host plant. *Ochrobactrum sp* CdSP9 had several PGPR traits such as ACC deaminase activity and Siderophore production (Pandey et al. 2013). *Ochrobactrum cytisi* IPA7.2 promotes the growth of potato microplants the resistant to abiotic stress (Burygin et al. 2019).

The genome of BU72 also contained several genes involved in defense mechanisms including, Osmotic stress (16), Oxidative stress (33), Resistance to antibiotics and toxic compounds (35).

Conclusion

In conclusion, *Brucella* BU72 strain showed the ability to grow on multiple hydrocarbons as sole energy and carbon sources, and to highly tolerate heavy metals. BU72 was able to produce different exopolysaccharide-based surfactants (EBS) when grown with glucose or with crude oil as sole carbon source. The analysis of the draft genome sequence confirmed the presence of genes involved in heavy metals resistance, EPS production and plant-growth promoting activities which suggest that BU72 may be a good candidate bioremediation and agriculture. activities in plant-growth promoting. Additionally, further research and testing are often necessary to optimize and validate the EPS production and the effectiveness of the application of BU72 in bioremediation.

Declarations

Author contribution

Conceived and designed the experiments: Mouna Mahjoubi, Habib Chouchane and Habibu Aliyu. Contributed reagents/materials/analysis tools: Mouna Mahjoubi, Habibu Aliyu, Simone Cappello, Hanene Cherif, Francesca

References

1. Alegbeleye OO, Opeolu BO, Jackson V (2017) Bioremediation of polycyclic aromatic hydrocarbon (PAH) compounds:(acenaphthene and fluorene) in water using indigenous bacterial species isolated from the Diep and Plankenburg rivers, Western Cape, South Africa. Brazilian journal of microbiology 48: 314-325. https://doi.org/10.1016/j.bjm.2016.07.027.

2. Aspedon A, Palmer K, Whiteley M (2006) Microarray analysis of the osmotic stress response in Pseudomonas aeruginosa. Journal of bacteriology 188: 2721 2725. https://doi.org/10.1128/jb.188.7.2721-2725.2006.

3. Aziz RK, Bartels D, Best AA, DeJongh M, Disz T, Edwards RA, Formsma K, Gerdes S, Glass EM, Kubal M (2008) The RAST Server: rapid annotations using subsystems technology. BMC genomics 9: 1-15. https://doi.org/10.1186/1471-2164-9-75.

4. Bankevich A, Nurk S, Antipov D, Gurevich AA, Dvorkin M, Kulikov AS, Lesin VM, Nikolenko SI, Pham S, Prjibelski AD (2012) SPAdes: a new genome assembly algorithm and its applications to single-cell sequencing. Journal of computational biology 19: 455-477. https://doi.org/10.1089/cmb.2012.0021.

5. Blin K, Shaw S, Augustijn HE, Reitz ZL, Biermann F, Alanjary M, Fetter A, Terlouw BR, Metcalf WW, Helfrich EJ (2023) antiSMASH 7.0: New and improved predictions for detection, regulation, chemical structures and visualisation. Nucleic acids research gkad344. https://doi.org/10.1093/nar/gkad344.

6. Burygin GL, Kargapolova KY, Kryuchkova YV, Avdeeva ES, Gogoleva NE, Ponomaryova TS, Tkachenko OV (2019) Ochrobactrum cytisi IPA7. 2 promotes growth of potato microplants and is resistant to abiotic stress. World Journal of Microbiology and Biotechnology 35: 1-12. https://doi.org/10.1007/s11274-019-2633-x.

7. Castellane TCL, Campanharo JC, Colnago LA, Coutinho ID, Lopes ÉM, Lemos MVF, de Macedo Lemos EG (2017) Characterization of new exopolysaccharide production by Rhizobium tropici during growth on hydrocarbon substrate. International journal of biological macromolecules 96: 361-369. https://doi.org/10.1016/j.ijbiomac.2016.11.123.

8. Castresana J (2000) Selection of conserved blocks from multiple alignments for their use in phylogenetic analysis. Molecular biology and evolution 17: 540-552. https://doi.org/10.1093/oxfordjournals.molbev.a026334.

9. Chai L-j, Jiang X-w, Zhang F, Zheng B-w, Shu F-c, Wang Z-l, Cui Q-f, Dong H-p, Zhang Z-z, Hou D-j (2015) Isolation and characterization of a crude oil degrading bacteria from formation water: comparative genomic analysis of environmental Ochrobactrum intermedium isolate versus clinical strains. Journal of Zhejiang University-SCIENCE B 16: 865-874. https://doi.org/10.1631/jzus.B1500029.

10. Chen I. M. A, Chu K, Palaniappan K, Ratner A, Huang J, Huntemann M., Patrick H, Stephan J, Cody W, Dongying W, Neha T B K, Supratim M, Galina O Matt N, Rekha S, Simon R, Axel V, Tanja W, Emiley A E, Nikos K, Ivanova, N. N (2023) The IMG/M data management and analysis system v. 7: content updates and new features. Nucleic Acids Research, 51(D1), D723-D732. https://doi.org/10.1093/nar/gkac976.

11. Cho S-H, Lee E, Ko S-R, Jin S, Song Y, Ahn C-Y, Oh H-M, Cho B-K, Cho S (2020) Elucidation of the biosynthetic pathway of vitamin B groups and potential secondary metabolite gene clusters via genome analysis of a marine bacterium Pseudoruegeria sp. M32A2M. Journal of Microbiology and Biotechnology 30: 505. https://doi.org/10.4014/jmb.1911.11006.

12. Chouchane H, Mahjoubi M, Ettoumi B, Neifar M, Cherif A (2018) A novel thermally stable heteropolysaccharide-based bioflocculant from hydrocarbonoclastic strain Kocuria rosea BU22S and its application in dye removal. Environmental technology 39: 859-872. https://doi.org/10.1080/09593330.2017.1313886.

13. Chouchane H, Boutiti S, Ouertani A, Hassen W, Guesmi S, Neifar M, Haikel J, Haïtham S, Ahmed S Masmoudi A S, Cherif A (2021) Effect of gamma irradiation on enhanced biological activities of exopolysaccharide from Halomonas desertis G11: Biochemical and genomic Insights. Polymers, 13(21), 3798. https://doi.org/10.3390/polym13213798.

14. Chudasama KS, Thaker VS (2017) Genome sequence of Ochrobactrum anthropi strain SUBG007, a plant pathogen and potential xenobiotic compounds degradation bacterium. Genomics data 11: 116-117. https://doi.org/10.1016/j.gdata.2017.01.001.

15. Crisafi F, Genovese M, Smedile F, Russo D, Catalfamo M, Yakimov M, Giuliano L, Denaro R (2016) Bioremediation technologies for polluted seawater sampled after an oil-spill in Taranto Gulf (Italy): A comparison of biostimulation, bioaugmentation and use of a washing agent in microcosm studies. Marine pollution bulletin 106: 119-126. https://doi.org/10.1016/j.marpolbul.2016.03.017.

16. D'Souza-Ault M, Smith LT, Smith G (1993) Roles of N-acetylglutaminylglutamine amide and glycine betaine in adaptation of Pseudomonas aeruginosa to osmotic stress. Applied and environmental microbiology 59: 473-478. https://doi.org/10.1128/aem.59.2.473-478.1993.

17. Ghosal D, Ghosh S, Dutta TK & Ahn Y (2016) Current state of knowledge in microbial degradation of polycyclic aromatic hydrocarbons (PAHs): a review. Frontiers in microbiology 1369. https://doi.org/10.3389/fmicb.2016.01369.

18. Grant JR, Enns E, Marinier E, Mandal A, Herman EK, Chen C-y, Graham M, Van Domselaar G, Stothard P (2023) Proksee: in-depth characterization and visualization of bacterial genomes. Nucleic Acids Research gkad326. https://doi.org/10.1093/nar/gkad326.

19. Gupta P, Diwan B (2017) Bacterial exopolysaccharide mediated heavy metal removal: a review on biosynthesis, mechanism and remediation strategies. Biotechnology Reports 13: 58-71. https://doi.org/10.1016/j.btre.2016.12.006.

20. Head IM, Jones DM, Röling WF (2006) Marine microorganisms make a meal of oil. Nature Reviews Microbiology 4: 173-182. https://doi.org/10.1038/nrmicro1348.

21. Hördt A, López MG, Meier-Kolthoff JP, Schleuning M, Weinhold L-M, Tindall BJ, Gronow S, Kyrpides NC, Woyke T, Göker M (2020) Analysis of 1,000+ type-strain genomes substantially improves taxonomic classification of Alphaproteobacteria. Frontiers in microbiology 11: 468. https://doi.org/10.3389/fmicb.2020.00468.

22. Huber B, Scholz HC, Kämpfer P, Falsen E, Langer S, Busse H-J (2010) Ochrobactrum pituitosum sp. nov., isolated from an industrial environment. International journal of systematic and evolutionary microbiology 60: 321-326. https://doi.org/10.1099/ijs.0.011668-0.

23. Huerta-Cepas J, Forslund K, Coelho LP, Szklarczyk D, Jensen LJ, Von Mering C, Bork P (2017) Fast genome-wide functional annotation through orthology assignment by eggNOG-mapper. Molecular biology and evolution 34: 2115-2122. https://doi.org/10.1093/molbev/msx148.

24. Ibrahim IM, Konnova SA, Sigida EN, Lyubun EV, Muratova AY, Fedonenko YP, Elbanna K (2020) Bioremediation potential of a halophilic Halobacillus sp. strain, EG1HP4QL: Exopolysaccharide production, crude oil degradation, and heavy metal tolerance. Extremophiles 24: 157-166. https://doi.org/10.1007/s00792-019-01143-2.

25. Jamal MT, Pugazhendi A (2018) Degradation of petroleum hydrocarbons and treatment of refinery wastewater under saline condition by a halophilic bacterial consortium enriched from marine environment (Red Sea), Jeddah, Saudi Arabia. 3 Biotech 8: 1-10. https://doi.org/10.1007/s13205-018-1296-x.

26. Kappell AD, Wei Y, Newton RJ, Van Nostrand JD, Zhou J, McLellan SL, Hristova KR (2014) The polycyclic aromatic hydrocarbon degradation potential of Gulf of Mexico native coastal microbial communities after the Deepwater Horizon oil spill. Frontiers in Microbiology 5: 205. https://doi.org/10.3389/fmicb.2014.00205.

27. Kimes NE, Callaghan AV, Suflita JM, Morris PJ (2014) Microbial transformation of the Deepwater Horizon oil spill—past, present, and future perspectives. Frontiers in Microbiology 5: 603. https://doi.org/10.3389/fmicb.2014.00603.

28. Kotecka K, Kawalek A, Kobylecki K, Bartosik AA (2021) The MarR-type regulator PA3458 is involved in osmoadaptation control in Pseudomonas aeruginosa. International Journal of Molecular Sciences 22: 3982. https://doi.org/10.3390/ijms22083982.

29. Lee I, Ouk Kim Y, Park S-C, Chun J (2016) OrthoANI: an improved algorithm and software for calculating average nucleotide identity. International journal of systematic and evolutionary microbiology 66: 1100-1103. https://doi.org/10.1099/ijsem.0.000760.

30. Lee SA, Sang MK, Song J, Kwon S-W, Weon H-Y (2020) Complete genome sequence of Brucella anthropi strain T16R-87 isolated from tomato (Solanum lycopersicum L.) rhizosphere. The Microbiological Society of Korea 56: 430-432. https://doi.org/10.7845/kjm.2020.0116.

31. Logeshwaran P, Megharaj M, Chadalavada S, Bowman M, Naidu R (2018) Petroleum hydrocarbons (PH) in groundwater aquifers: An overview of environmental fate, toxicity, microbial degradation and risk-based remediation approaches. Environmental technology & innovation 10: 175-193. https://doi.org/10.1016/j.eti.2018.02.00.

32. Mahjoubi M, Cappello S, Souissi Y, Jaouani A, Cherif A (2018) Microbial bioremediation of petroleum hydrocarbon−contaminated marine environments. Recent Insights in Petroleum Science and Engineering; Zoveidavianpoor, M, Ed 325-350. https://doi.org/10.5772/intechopen.72207.

33. Mahjoubi M, Aliyu H, Neifar M, Cappello S, Chouchane H, Souissi Y, Masmoudi AS, Cowan DA, Cherif A (2021) Genomic characterization of a polyvalent hydrocarbonoclastic bacterium Pseudomonas sp. strain BUN14. Scientific Reports 11: 8124. https://doi.org/10.1038/s41598-021-87487-2.

34. Mahjoubi M, Jaouani A, Guesmi A, Amor SB, Jouini A, Cherif H, Najjari A, Boudabous A, Koubaa N, Cherif A (2013) Hydrocarbonoclastic bacteria isolated from petroleum contaminated sites in Tunisia: isolation, identification and characterization of the biotechnological potential. New biotechnology 30: 723-733. https://doi.org/10.1016/j.nbt.2013.03.004.

35. Moens M, Branco R, Morais PV (2020) Arsenic accumulation by a rhizosphere bacterial strain Ochrobactrum tritici reduces rice plant arsenic levels. World Journal of Microbiology and Biotechnology 36: 1-11. https://doi.org/10.1007/s11274-020-2800-0.

36. Mohite BV, Koli SH, Narkhede CP, Patil SN, Patil SV (2017) Prospective of microbial exopolysaccharide for heavy metal exclusion. Applied biochemistry and biotechnology 183: 582-600. https://doi.org/10.1007/s12010-017-2591-4.

37. Nayak T, Panda AN, Adhya TK, Das B, Raina V (2019) Biodegradation of Chlorpyrifos and 3, 5, 6-trichloro-2-pyridinol (TCP) by Ochrobactrum sp. CPD-03: Insights from genome analysis on organophosphorus pesticides degradation, chemotaxis and PGPR activity. BioRxiv 2019.2012. 2012.866210. https://doi.org/10.1101/2019.12.12.866210.

38. Onder Erguven G, Demirci U (2020) Statistical evaluation of the bioremediation performance of Ochrobactrum thiophenivorans and Sphingomonas melonis bacteria on Imidacloprid insecticide in artificial agricultural field. Journal of Environmental Health Science and Engineering 18: 395-402. https://doi.org/10.1007/s40201-019-00391-w.

39. Ortega-Gonzalez DK, Cancino-Diaz JC, Zaragoza D, Flores-Ortiz CM, Cruz-Maya JA, Jan-Roblero J (2018) Ochrobactrum anthropi BPyF3: Naphthalene biodegradation and the involvement of dioxygenase. Romanian Biotechnological Letters 23: 13310.

40. Ouertani R, Ouertani A, Mahjoubi M, Bousselmi Y, Najjari A, Cherif H, Chamkhi A, Mosbah A, Khdhira H, Sghaier H, Chouchane H, Cherif A, Neifar M (2020) New plant growth-promoting, chromium-detoxifying microbacterium species isolated from a tannery wastewater: performance and genomic insights. Frontiers in Bioengineering and Biotechnology 8: 521. https://doi.org/10.3389/fbioe.2020.00521.

41. Ozdemir G, Ozturk T, Ceyhan N, Isler R, Cosar T (2003) Heavy metal biosorption by biomass of Ochrobactrum anthropi producing exopolysaccharide in activated sludge. Bioresource technology 90: 71-74. https://doi.org/10.1016/S0960-8524(03)00088-9.

42. Pal S, Kundu A, Banerjee TD, Mohapatra B, Roy A, Manna R, Sar P, Kazy SK (2017) Genome analysis of crude oil degrading Franconibacter pulveris strain DJ34 revealed its genetic basis for hydrocarbon

degradation and survival in oil contaminated environment. Genomics 109: 374-382. https://doi.org/10.1016/j.ygeno.2017.06.002.

43. Pandey S, Ghosh PK, Ghosh S, De TK, Maiti TK (2013) Role of heavy metal resistant Ochrobactrum sp. and Bacillus spp. strains in bioremediation of a rice cultivar and their PGPR like activities. Journal of Microbiology 51: 11-17. https://doi.org/10.1007/s12275-013-2330-7

44. Peng H, Xie W, Li D, Wu M, Zhang Y, Xu H, Ye J, Ye T, Xu L, Liang Y (2019) Copper-resistant mechanism of Ochrobactrum MT180101 and its application in membrane bioreactor for treating electroplating wastewater. Ecotoxicology and Environmental Safety 168: 17-26. https://doi.org/10.1016/j.ecoenv.2018.10.066.

45. Qian Z, Wu C, Pan W, Xiong X, Xia L, Li W (2022) Arsenic transformation in soil-rice system affected by iron-oxidizing strain (Ochrobactrum sp.) and related soil metabolomics analysis. Frontiers in Microbiology 13: 794950. https://doi.org/10.3389/fmicb.2022.794950.

46. Ramasamy S, Mathiyalagan P, Chandran P (2014) Characterization and optimization of EPS-producing and diesel oil-degrading Ochrobactrum anthropi MP3 isolated from refinery wastewater. Petroleum Science 11: 439-445. https://doi.org/10.1007/s12182-014-0359-9.

47. Ryan MP, Pembroke JT (2020) The genus Ochrobactrum as major opportunistic pathogens. Microorganisms 8: 1797. https://doi.org/10.3390/microorganisms8111797.

48. Santisi S, Cappello S, Catalfamo M, Mancini G, Hassanshahian M, Genovese L, Giuliano L, Yakimov MM (2015) Biodegradation of crude oil by individual bacterial strains and a mixed bacterial consortium. Brazilian Journal of Microbiology 46: 377-387. https://doi.org/10.1590/S1517-838246120131276.

49. Santisi S, Cappello S, Catalfamo M, Mancini G, Hassanshahian M, Genovese L, Giuliano L, Yakimov MM (2015) Biodegradation of crude oil by individual bacterial strains and a mixed bacterial consortium. Brazilian Journal of Microbiology 46: 377-387. https://doi.org/10.1002/clen.200700042.

50. Sany SBT, Hashim R, Rezayi M, Salleh A, Rahman MA, Safari O, Sasekumar A (2014) Human health risk of polycyclic aromatic hydrocarbons from consumption of blood cockle and exposure to contaminated sediments and water along the Klang Strait, Malaysia. Marine pollution bulletin 84: 268-279. https://doi.org/10.1016/j.marpolbul.2014.05.004.

51. Sengupta D, Datta S, Biswas D (2020) Surfactant exopolysaccharide of Ochrobactrum pseudintermedium C1 has antibacterial potential: Its bio-medical applications in vitro. Microbiological research 236: 126466. https://doi.org/10.1016/j.micres.2020.126466.

52. Stanton S, Meyer JJM, Van der Merwe CF (2013) An evaluation of the endophytic colonies present in pathogenic and non-pathogenic Vanguerieae using electron microscopy. South African journal of botany 86: 41-45. https://doi.org/10.1016/j.sajb.2013.01.007.

53. Talwar M, Mulla S & Ninnekar H (2014) Biodegradation of organophosphate pesticide quinalphos by Ochrobactrum sp. strain HZM. Journal of applied microbiology 117: 1283-1292. https://doi.org/10.1111/jam.12627.

54. Tamura K, Stecher G, Peterson D, Filipski A, Kumar S (2013) MEGA6: molecular evolutionary genetics analysis version 6.0. Molecular biology and evolution 30: 2725-2729. https://doi.org/10.1093/molbev/mst197.

55. Tormoehlen L, Tekulve K, Nañagas K (2014) Hydrocarbon toxicity: a review. Clinical toxicology 52: 479-489. https://doi.org/10.3109/15563650.2014.923904.

56. Yagel Y, Sestito S, Motro Y, Shnaiderman-Torban A, Khalfin B, Sagi O, Navon-Venezia S, Steinman A, Moran-Gilad J (2020) Genomic characterization of antimicrobial resistance, virulence, and phylogeny of the genus Ochrobactrum. Antibiotics 9: 177. https://doi.org/10.3390/antibiotics9040177.

57. Yang Y, Yu X, Zhang R (2013) Draft genome sequence of Ochrobactrum pseudogrignonense strain CDB2, a highly efficient arsenate-resistant soil bacterium from arsenic-contaminated cattle dip sites. Genome announcements 1. https://doi.org/10.1128/genomea.00173-13.

58. Yaşar Yildiz S, Nikerel E, Toksoy Öner E (2019) Genome-Scale Metabolic Model of a Microbial Cell Factory (Brevibacillus thermoruber 423) with Multi-Industry Potentials for Exopolysaccharide Production. OMICS: A Journal of Integrative Biology 23: 237-246. https://doi.org/10.1089/omi.2019.0028.

59. Yirui W, Tengteng H, Zhong M, Zhang Y, Enmin L, Huang T, Zhong H (2009) Isolation of marine benzo [a] pyrene-degrading Ochrobactrum sp. BAP5 and proteins characterization. Journal of Environmental Sciences 21: 1446-1451. https://doi.org/10.1016/S1001-0742(08)62438-9.

60. Yoon S-H, Ha S-M, Kwon S, Lim J, Kim Y, Seo H, Chun J (2017) Introducing EzBioCloud: a taxonomically united database of 16S rRNA gene sequences and whole-genome assemblies. International journal of systematic and evolutionary microbiology 67: 1613. https://doi.org/10.1099/ijsem.0.001755.

61. Yu Z, Sui Y, Peng S, Li T, Phanpadith P (2019) Ochrobactrum pituitosum causes kernel rot and premature shedding of fresh walnut fruits. International Journal of Agriculture and Biology 22: 497-502. ttps://doi.org/10.1099/ijsem.0.001755.

62. Zarinviarsagh M, Ebrahimipour G, Sadeghi H (2017) Lipase and biosurfactant from Ochrobactrum intermedium strain MZV101 isolated by washing powder for detergent application. Lipids in health and disease 16: 177. https://doi.org/10.1186/s12944-017-0565-8.

63. Ziervogel K, Joye SB, Kleindienst S, Malkin SY, Passow U, Steen AD, Arnosti C (2019) Polysaccharide hydrolysis in the presence of oil and dispersants: Insights into potential degradation pathways of exopolymeric substances (EPS) from oil-degrading bacteria. Elem Sci Anth 7. https://doi.org/10.1525/elementa.371.f4.
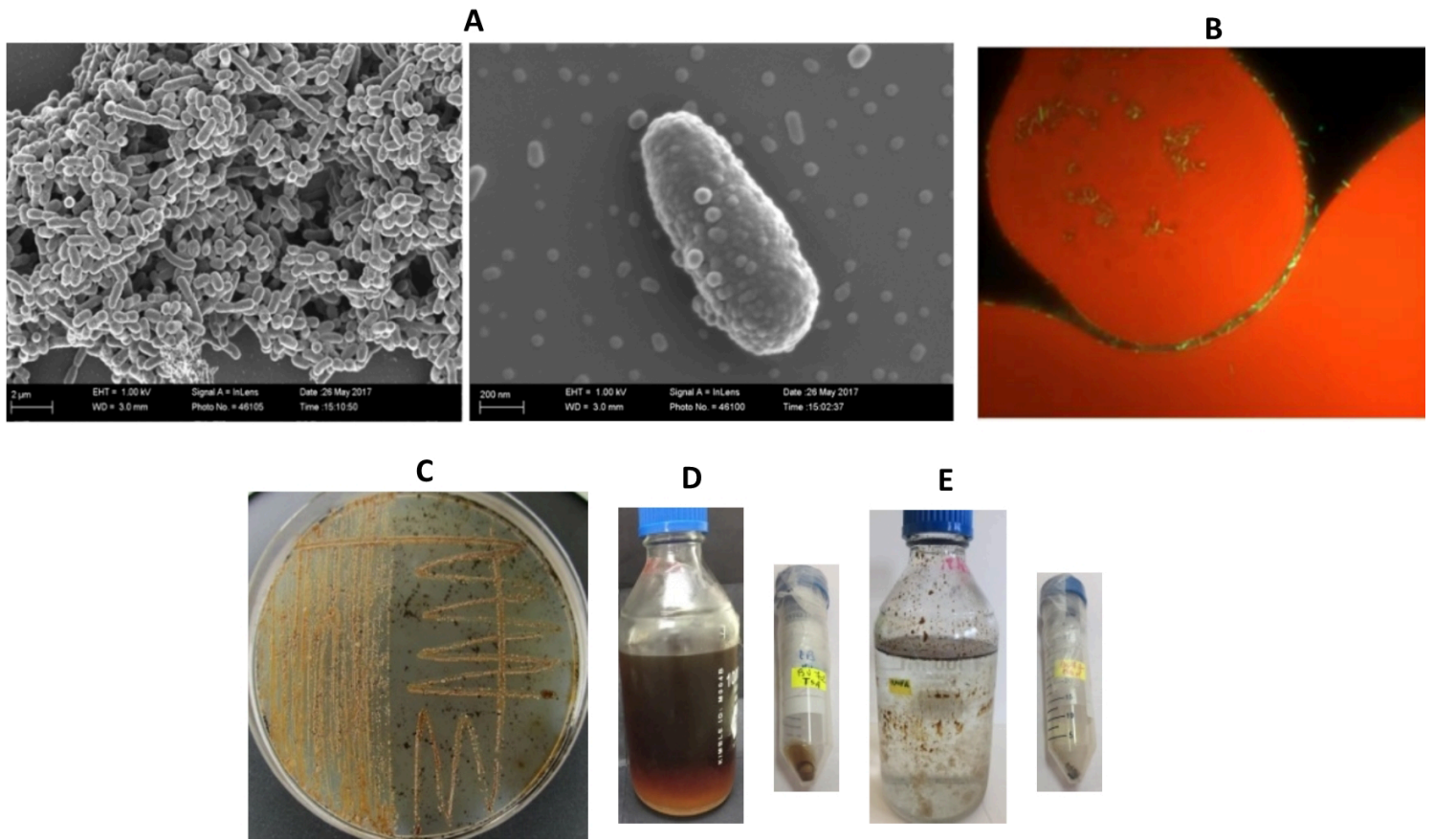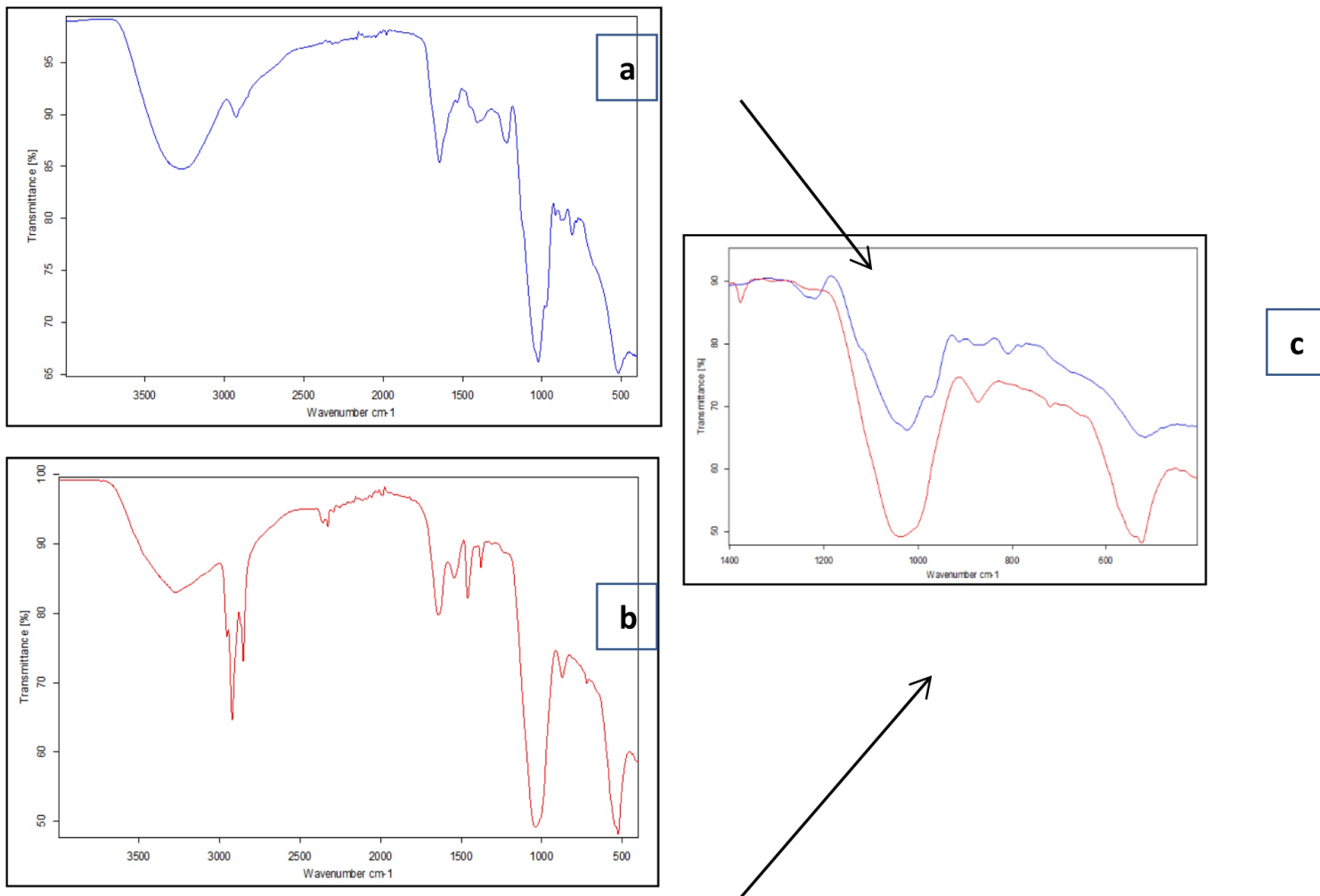
Figures
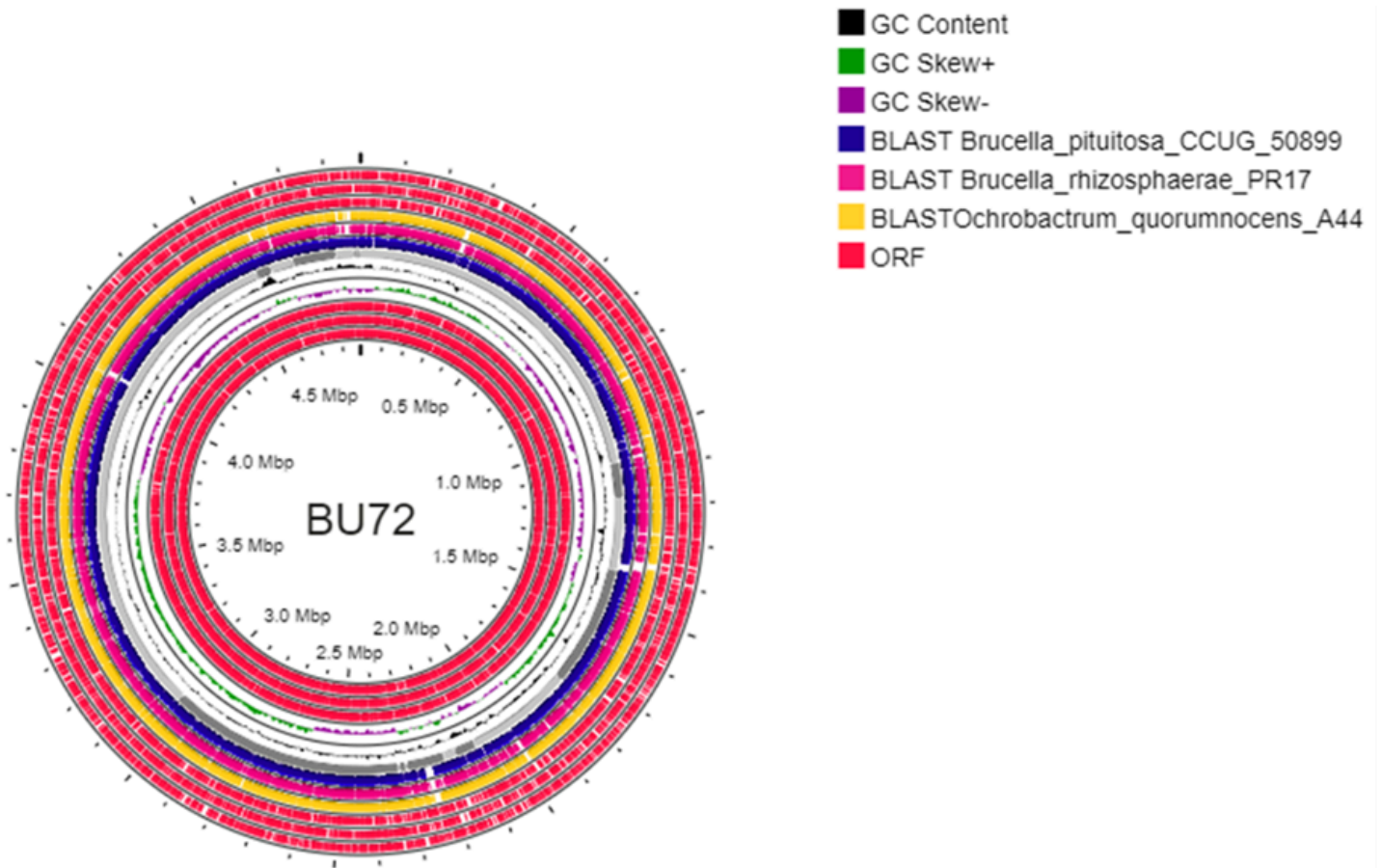
Figure 1

A) Scanning electron micrograph (SEM) showing Rod-shape cell morphology of *Brucella pituitosa* strain BU72. B- Epifluorescence microscopy image of the green rod shape cells of the GFP-tagged *Brucella pituitosa* BU72-GFP mutant. The red spot are due to the background fluorescence of diesel droplets under the selected wavelength of fluorescent light. C) Growth of the strain BU72 in ONR7a medium supplemented with 1% crude oil. D) EPS produced by BU72 in TSA + glucose; D) EPS produced by BU72 in ONR7a + 1% crude oil B- Epifluorescence microscopy image of the green rod shape cells of the GFP-tagged *Brucella pituitosa* BU72-GFP mutant. The red spots are due to the background fluorescence of diesel droplets under the selected wavelength of fluorescent light.

Figure 2

FTIR Spectra of EPS obtained with, **a**) glucose used as carbon source, **b**) crude oil used as carbon source, and **c**) comparison of the functional groups in the characteristic region of the molecular fingerprint (1400-400 cm^{-1}) of both EPS. A strong absorption peaks at 3250 cm^{-1} generated by -OH group (for both EBS). The absorbance peaks in the region 2900–2700 cm^{-1} (b) and at 2800 cm^{-1} (a)
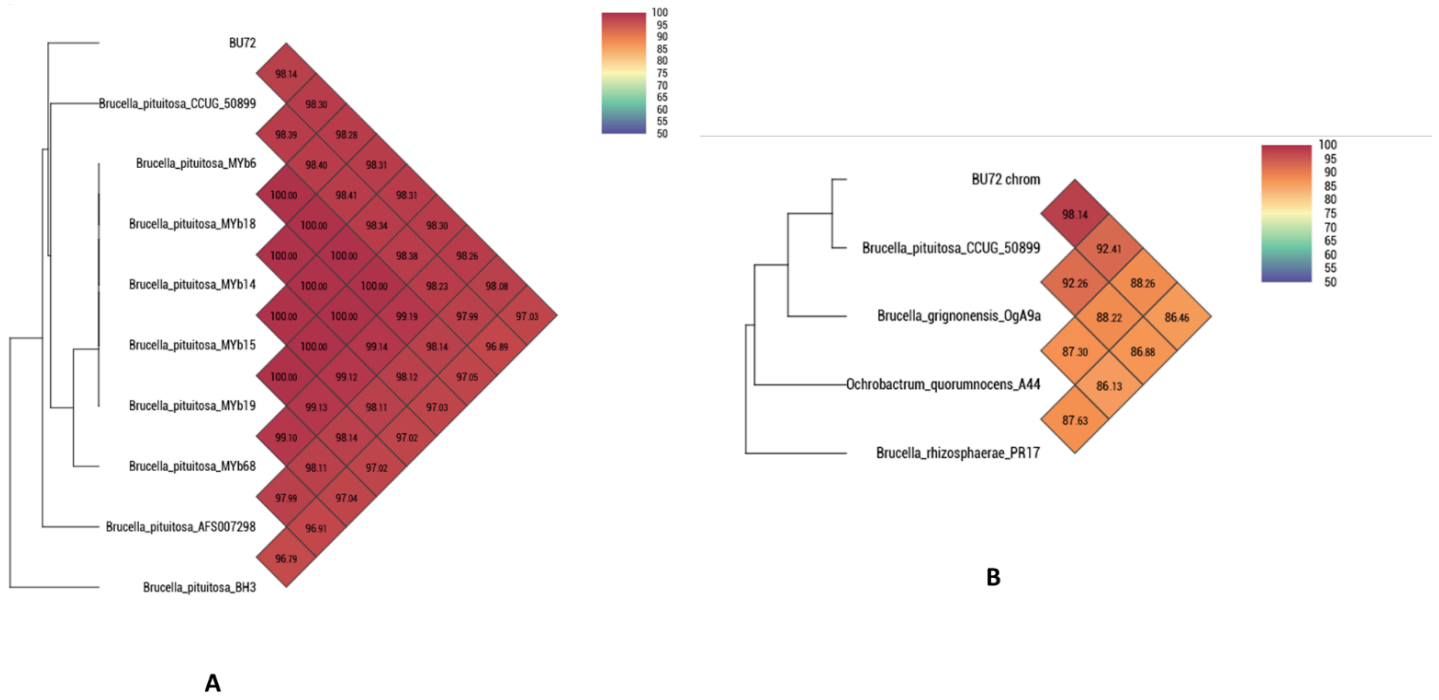
Figure 3

Circular representation of the BU72 genome using Proksee (https://proksee.ca). The innermost rings depict GC content (Black) and GC Skew (purple/green). The outermost rings depict genomes of the closest type strain to BU72: *Brucella pituitosa* CCUG_50899 (blue), *Brucella rhizosphaerae* PR17 (Pink) and *Ochrobactrum quorumnocens* A44 (Yellow) according to BLAST identity. The ORF are shown with red color.
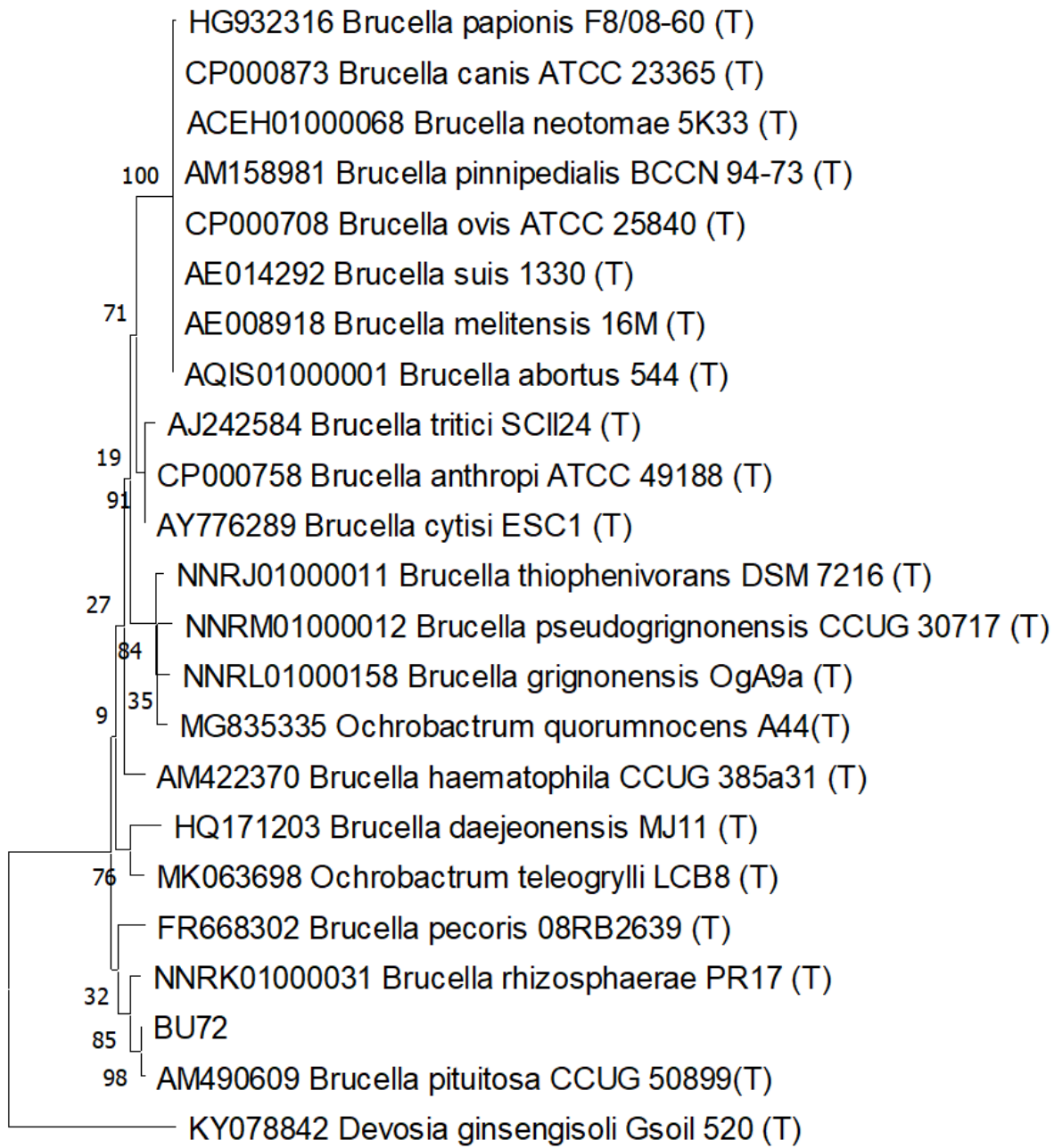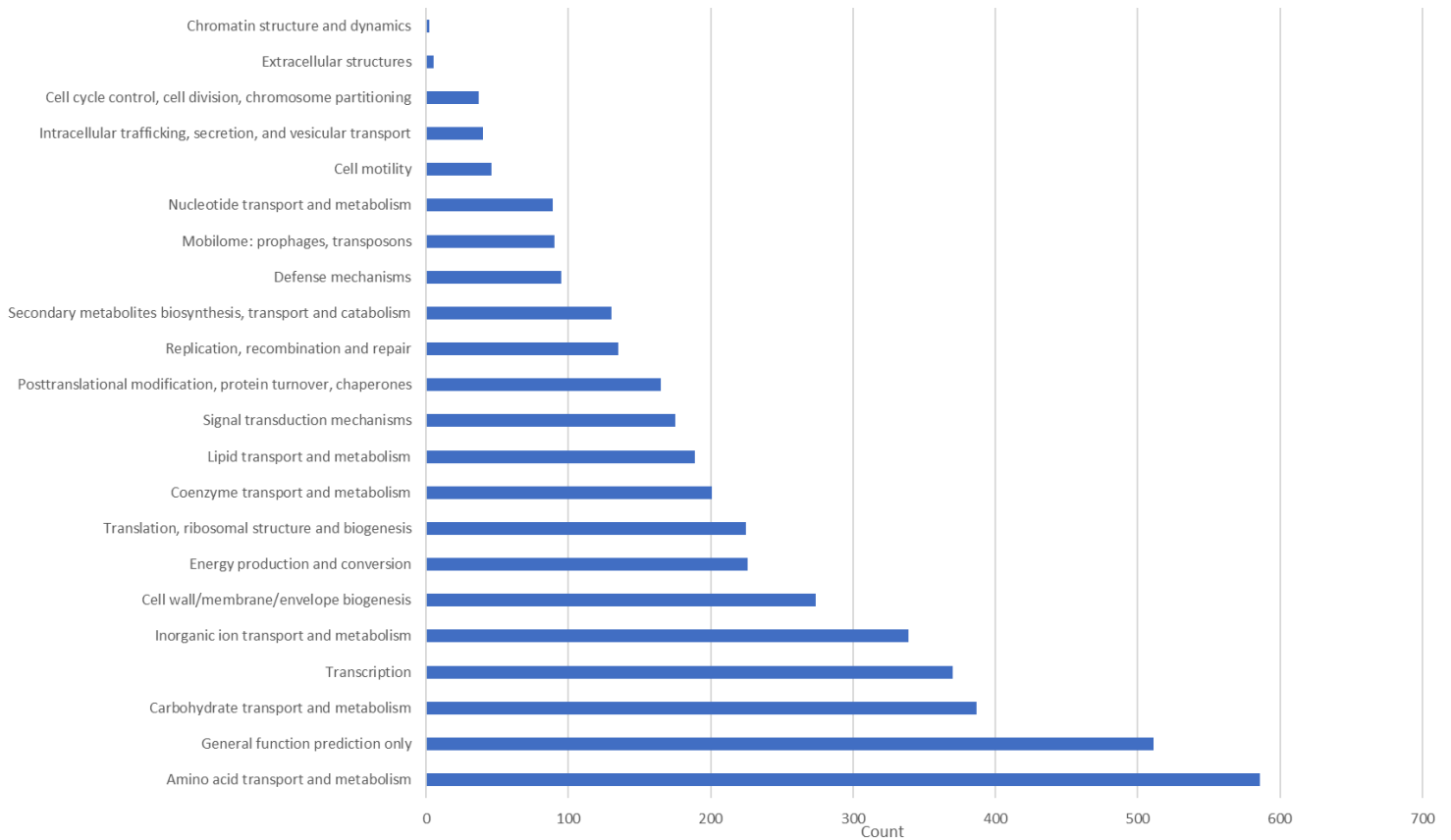
Figure 4

Phylogenetic analysis of 16S rRNA gene sequence of strain BU72 and most closely related *Brucella* type strains. The phylogeny neighbor joining tree was evaluated by performing bootstrap analysis of 1000 data sets using MEGA6.06.

Figure 5

Heatmap of average nucleotide identity (ANI) values between, **A**) BU72 and available *Brucella pituitosa* genomes,; **B**) BU 72 and its closest relatives Brucella strains . Heatmap was generated by OAT

Figure 6

Number of genes associated with general COG functional categories

Supplementary Files

This is a list of supplementary files associated with this preprint. Click to download.

- SupplementaryinformationsMahjoubietal2023.docx